

Transmission of SARS in dynamical small-world networks

Naoki Masuda,¹ Norio Konno,¹ and Kazuyuki Aihara^{2,3}

¹*Faculty of Engineering, Yokohama National University,
79-5, Tokiwadai, Hodogaya, Yokohama, 240-8501 Japan*

²*Department of Complexity Science and Engineering,
Graduate School of Frontier Sciences, University of Tokyo,*

7-3-1 Hongo Bunkyo-ku Tokyo 113-8656 Japan

³*ERATO Aihara Complexity Modelling Project,
Japan Science and Technology Agency, Tokyo, Japan*

(Dated: February 8, 2020)

Abstract

The outbreak of Severe Acute Respiratory Syndrome (SARS) is still threatening the world because of a possible resurgence. In the current situation that effective medical treatments such as antiviral drugs are not discovered yet, dynamical features of the epidemics should be clarified for establishing strategies for tracing, quarantine, isolation, and regulating social behavior of the public at appropriate costs. Here we propose a network model for SARS epidemics and discuss why super-spreaders emerged and why SARS spread especially in hospitals, which were key factors of the recent outbreak. We suggest that super-spreaders are biologically contagious patients, and they may amplify the spreads by going to potentially contagious places such as hospitals. To avoid mass transmission in hospitals, it may be a good measure to treat suspected cases without hospitalizing them. Finally, we indicate that SARS probably propagates in small-world networks associated with human contacts, and that biological nature of individuals and social group properties are factors more important than heterogeneous rates of social contacts among individuals. This is in marked contrast with epidemics of sexually transmitted diseases (STD) or computer viruses to which scale-free network models often apply.

I. INTRODUCTION

The first case of the recent outbreak of Severe Acute Respiratory Syndrome (SARS) is estimated to have started in the Guangdong province of the People's Republic of China in November of 2002. After that SARS spread to many countries, causing a number of infectious cases. In spite of worldwide research efforts, the biological mechanism of the SARS infection is not yet fully clarified, which mars developments of antiviral drugs or other means of conclusive medication. Under this condition, an effective way was to track everybody suspected to be involved in the spreads and quarantine them, which is the same as a century ago. However, more effective strategies in terms of safety and cost could be established with the knowledge of dynamical mechanisms of the outbreak including the effects of so called super-spreaders (SSs) and spreads in hospitals. Along this line, epidemiological models that explain the actual and potential transmission patterns can be helpful for suppressing the spreads. For example, dynamical compartmental models for fully mixed population [1] and for geographical subpopulations in Hong Kong [2] have been proposed and fitted to the real data, and they are successful in explaining the real data and determining the basic reproductive number [3]. However, the models contain many compartments and many parameters whose values are determined manually, which may obscure relative contributions of the factors. Here we rather propose a simplified spatial model to indicate how interplay between network structure and individual factors affects the epidemics.

A prominent feature in the SARS epidemics is the dominant influence of SSs [1, 2, 4]. According to Centers for Disease Control and Prevention (CDC) of the USA, a patient is defined to be SS if he/she has infected more than 10 people. The SARS epidemics are special in that a majority of cases originated from just a small number of SSs. On the other hand, non-super-spreading patients, which by far outnumber SSs, explain only a small portion of the infection events. In Singapore, just 5 SSs have infected 80% of about two hundreds of patients, whereas about 80% of the patients have infected nobody [4, 5, 6]. Also in Hong Kong, one patient caused more than hundred successive cases [2, 6]. Similar key persons are identified in other parts of the world as well. Also epidemics of Ebola, measles, and tuberculosis often accompany SSs [4]. It is

believed that SSs are caused both by biological reasons such as genetic tendencies, health conditions, and strength of the virus, and by social reasons such as the manner of social contacts and global structure of social interaction. It agrees with general understanding that epidemics depend on the personal factors and the structure of social networks [7, 8]. Although previous dynamical models consider SSs to be exceptional [2] or do not model them explicitly [1], we incorporate them as a key factor for the spreading.

Another feature of SARS is rapid spreading in hospitals, which played a pivotal role in, at least, local outbreaks, sometimes accounting for more than half the total regional cases. The embarrassing fact that hospitals are actually amplifying diseases [2, 4] should be provided with convincing mechanisms so that we can reduce the risk of spreads in hospitals and relieve the public of anxieties. To this end again, we will examine the combined effects of SSs and network structure.

Here we construct a dynamical model for SARS spreads, which is simpler than the previous models [1, 2] but takes into account SSs and the spatial structure represented by the small-world properties [9]. We then propose possible means for preventing SARS spreads in the absence of vaccination. The simulated SARS epidemics are also compared with the epidemics of STDs and computer viruses whose mechanism owes much to scale-free properties of the underlying networks [8, 10, 11, 12].

II. MODEL AND GENERAL THEORY

Our model is composed of n persons located on vertices of a graph. A pair of individuals connected by an undirected edge directly interact and possibly transmit SARS. We simply assume three types of individuals, namely, the susceptible, the infected but non-SSs, and the SSs. Here a SS, probably with strong and/or a large amount of viruses, has a strong tendency to infect the susceptible, even without frequent social contacts. The dynamics is the contact process with three states [12, 13, 14]. A susceptible can be infected by an adjacent patient (a SS or an infected non-SS) at certain rates. A patient returns to the susceptible state at rate 1, mimicking the recovery from SARS or its death followed by the local emergence of a new healthy person. The infected non-SSs and SSs are modeled with different rates of infection [3, 8, 14]. An

infected turns an adjacent susceptible into infected non-SS or SS at rate $\lambda_I(1 - p)$ or $\lambda_I p$, respectively, where p parameterizes the number of SSs divided by the number of patients. Similarly, a SS infects an adjacent susceptible into infected non-SS or SS at rate $\lambda_{SS}(1 - p)$ or $\lambda_{SS} p$, respectively [14]. The infected non-SSs and SSs do not have direct interactions even if they are next to each other. However, they interact indirectly owing to the crosstalk rates $\lambda_I p$ and $\lambda_{SS}(1 - p)$. These infection events as well as death events at rate 1 happen independently for all the sites. The parameter values depend on the definition of SS, the network structure, and the time scales. With the supposition of total mixing of the individuals and the definition of SS by CDC, the data of the outbreak in Singapore [4] provide a rough estimate of $p = 0.03$. As a rough estimation, we set $\lambda_{SS}/\lambda_I = 20$ based on the descriptions on a small number of super-spreaders identified in Singapore [4] and in Hong Kong [2, 6]. To our knowledge, larger data about the number of cases caused by each patient or about the detailed chains of transmissions are not available in other regions. A relevant condition that seemingly holds in the current outbreak is $\lambda_I < 1 < \lambda_{SS}$, where λ_I and λ_{SS} are multiplied by the number of neighbors for a moment. In this situation, the meanfield theory predicts the existence of a threshold for p above which the disease spreads widely [14]. The recent outbreak may have been led to a suprathreshold regime even with small p because λ_{SS} is presumably huge. The model studies using the real data suggest that the threshold has been crossed from the above by the control efforts [1, 2].

Next we introduce the local network structure. At a given time, the whole population is typically divided into groups within which relatively frequent social contacts are expected. A group represents, for example, hospital, school, family, market, train, and office, and it is characterized by clustering properties [9, 15] and dense coupling. We prepare g groups, each containing $n_g = n/g$ individuals. The i th individual ($1 \leq i \leq n$) is connected to randomly chosen k_i ($0 \leq k_i \leq n_g - 1$) individuals within the group. The rate of transmission is proportional to the vertex degree k_i in the early stage of epidemics [3, 12]. Apart from the effects of k_i , λ_I , and λ_{SS} , some social groups are more prone to transmit SARS than others. This group-dependency originates in, for example, ventilation, sanitary levels, and the duration of grouping [1, 2, 5]. The effect is represented by a multiplicative factor T_j for the j th group ($1 \leq j \leq g$). Then the effective intragroup infection strength is calculated as $\langle k_i \rangle_j T_j$, where $\langle \rangle_j$ is the average

over i in the j th group. Presumably, social groups such as hospitals, congested trains, airplanes, and poorly ventilated residences have large $\langle k_i \rangle_j T_j$. For example, hospitals may have large $\langle k_i \rangle_j T_j$ because of a high population density yielding large $\langle k_i \rangle_j$ and the fact that the susceptible hospitalized for other diseases may be generally weak against infectious diseases including SARS. The influence of trains due to congestion and closedness of the air for long time is a potential source of outbreaks in the regions where people habitually commute by congested public transportations, like Japan. In contrast, $\langle k_i \rangle_j T_j$ may be low for groups formed in open spaces. However, we note that SARS can also break out in low-risk groups if λ_{SS} is sufficiently large. For simplicity, we assume that g_0 out of g groups have $T_j = T_h$ that is larger than $T_j = T_l$ taken by the other $g - g_0$ groups.

Although many models ignore spatial structure of the population and rely on mean-field descriptions [1, 3], spatial aspects should be incorporated for understanding real dynamics of the epidemics [2, 7, 8, 16]. A mainstream from this standpoint is methods of percolation and contact process on regular lattices [13, 14, 17]. However, d -dimensional lattices have the characteristic path length L , that is, the mean distance between a pair of vertices, proportional to $n^{1/d}$. In social networks, L is approximately proportional to $\log n$ as in random graphs [9]. To cope with this observation, we introduce random recombination of n individuals into g new groups. In reality, one belongs to many groups that dynamically break and reform more or less randomly by way of social activities [7, 18]. For example, one may commute to one's workplace and return home everyday, possibly by changing trains, which serve as temporary social groups as well. After time t_0 , we randomly shuffle all the vertices and reorganize them into g groups and wire the vertices within each group in the same manner as before. Then the epidemic dynamics is run for another t_0 before next shuffling occurs. For simplicity, just two independent groupings are assumed to alternate, as schematically shown in Fig. 1. However, the results are easily extended to the case of longer chains of group reformation. Owing to the shuffling, individuals initially belonging to different groups can interact in the long run.

We denote $x_{\alpha,I}$ and $x_{\alpha,SS}$ the number of the infected non-SSs and that of the SSs summed over the groups with $T_j = T_\alpha$ ($\alpha = h, l$). In early stages of epidemics, the

dynamics between two switching events is given by the meanfield description as follows:

$$\frac{d}{dt} \begin{pmatrix} x_{h,SS} \\ x_{h,I} \\ x_{l,SS} \\ x_{l,I} \end{pmatrix} = \begin{pmatrix} \lambda_{SSp} \langle k_i \rangle_h T_h - 1 & \lambda_{Ip} \langle k_i \rangle_h T_h & 0 & 0 \\ \lambda_{SS(1-p)} \langle k_i \rangle_h T_h & \lambda_{I(1-p)} \langle k_i \rangle_h T_h - 1 & 0 & 0 \\ 0 & 0 & \lambda_{SSp} \langle k_i \rangle_l T_l - 1 & \lambda_{Ip} \langle k_i \rangle_l T_l \\ 0 & 0 & \lambda_{SS(1-p)} \langle k_i \rangle_l T_l & \lambda_{I(1-p)} \langle k_i \rangle_l T_l - 1 \end{pmatrix} \begin{pmatrix} x_{h,SS} \\ x_{h,I} \\ x_{l,SS} \\ x_{l,I} \end{pmatrix}, \quad (1)$$

where $\langle \rangle_\alpha$ denotes averaging over the groups with $T_j = T_\alpha$. The random shuffling is expressed by multiplication of the following matrix from the left:

$$\begin{pmatrix} \frac{g_0}{g} + \sigma & 0 & \frac{g_0}{g} + \sigma & 0 \\ 0 & \frac{g_0}{g} + \sigma & 0 & \frac{g_0}{g} + \sigma \\ \frac{g-g_0}{g} - \sigma & 0 & \frac{g-g_0}{g} - \sigma & 0 \\ 0 & \frac{g-g_0}{g} - \sigma & 0 & \frac{g-g_0}{g} - \sigma \end{pmatrix}, \quad (2)$$

where σ is the possible correlation factor specifying the tendency for patients to join groups with $\langle k_i \rangle_j T_j = \langle k_i \rangle_h T_h$. Purely random mixing yields $\sigma = 0$. The map for the one-round dynamics comprising the contact process for time t_0 followed by switching has eigenvalues 0, 0, $e^{-t_0} \cong 1 - t_0$, and $(\frac{g_0}{g} + \sigma) e^{(-1+T_h \langle k_i \rangle_h (\lambda_I(1-p) + \lambda_{SSp}))t_0} + (\frac{g-g_0}{g} - \sigma) e^{(-1+T_l \langle k_i \rangle_l (\lambda_I(1-p) + \lambda_{SSp}))t_0} \cong 1 + \left[\left(\frac{g_0}{g} + \sigma \right) T_h \langle k_i \rangle_h + \left(\frac{g-g_0}{g} - \sigma \right) T_l \langle k_i \rangle_l \right] (\lambda_I(1-p) + \lambda_{SSp}) - 1$ for t_0 small with respect to the system time t introduced in Eq. 1. An important indicator of outbreaks is the basic reproductive number R_0 defined as the mean number of secondary infections produced by a single patient in a susceptible population [1, 2, 3, 7, 8, 19]. If R_0 exceeds unity, the disease spreads on average in mixed populations such as the local groups in Fig. 1. Since R_0 equals the largest eigenvalue, what matters is whether $\left(\left(\frac{g_0}{g} + \sigma \right) T_h \langle k_i \rangle_h + \left(\frac{g-g_0}{g} - \sigma \right) T_l \langle k_i \rangle_l \right) (\lambda_I(1-p) + \lambda_{SSp})$ is greater than 1. As a result, multiple kinds of heterogeneities [3], namely, the factors associated with individual patients and those specific to the groups, interact and determine the tendency to spread. Generally speaking, a positive σ raises R_0 . Even if both factors are subthreshold in the absence of σ , that is, $\left(\frac{g_0}{g} T_h \frac{\langle k_i \rangle_h}{\langle k_i \rangle} + \frac{g-g_0}{g} T_l \frac{\langle k_i \rangle_l}{\langle k_i \rangle} \right) < 1$ and $(\lambda_I(1-p) + \lambda_{SSp}) \langle k_i \rangle < 1$, a positive σ can make the whole dynamics suprathreshold. In actual SARS spreads in hospitals, $\sigma > 0$ seems to have held; compared with healthy people, the SARS patients and the suspected are obviously more likely to go to hospital where T_j and $\langle k_i \rangle_j$ are supposedly high. Currently, we do not have control over infection rates of individuals, particularly, λ_{SS} [2]. However, the threat of spreads may be decreased if their behavior

is altered so that they avoid risky places. It is recommended that they be seen by doctor at home or some isolated sites. The strategies applied in many countries such as introducing more separated hospital rooms, making doctors and nurses work in a single ward [20], and ordering the public to stay home also decrease k_i and σ [2].

III. SIMULATION RESULTS

We next examine effects of network structure by numerical simulations. To focus on topological factors, we simply set $T_h = T_l = 1$ and $k_i = k = n_g - 1$ ($1 \leq i \leq n$). The group size n_g , which is typically somewhat smaller than 100 [18], is chosen to be $81 = 9^2$ for technical reasons, although the value really relevant to the SARS epidemics is not known [1]. With $g = 100$, $n = gn_g = 90^2$, and $t_0 = 0.5$, the chains of infection after the total run time $\bar{t} = 1.0$, from the viewpoint of two different groupings as in Fig. 1, are shown in Fig. 2(a, b). They more or less reproduce the transmission pattern of SARS in Singapore [4], including the rapid spreads mediated by small L and the massive influence of SSs (solid lines). The transmission naturally spreads over time, as shown in Fig. 2(c) corresponding to $\bar{t} = 2.0$. By comparing Fig. 2(c) with Fig. 2(d), which shows the results for $\bar{t} = 2.0$ and $t_0 = 1.0$, we find that local transmission develops if the time spent with a fixed group configuration is relatively longer.

More quantitatively, Fig. 3(a) shows, for $\bar{t} = 2.0$ and $t_0 = 0.5$, the distributions of a_i , which is the number of people to whom the i th patient has directly infected. The patients with large a_i are mostly SSs. Small a_i is chiefly covered by other patients, and the distribution decays exponentially in a_i within this range. The homogeneous vertex degree and the Poisson property of the processes caused the exponential tail, which is preserved in small-world-type networks like ours and random graphs [9] where the vertex degrees obey narrow distributions.

IV. DISCUSSION

A. Comparison with Regular Lattices

A time course of chains of infection in a two-dimensional square lattice are shown in Fig. 2(e, f, g), with n , g , k_i , and the duration of the run the same as before. We

assume the periodic boundary conditions, and $k_i = 80$ neighbors of a vertex (x,y) ($1 \leq x, y \leq 90$) are defined to be the vertices included in the square with center (x,y) and side length 9. The infection pattern appears similar to Fig. 2(a, b, c, d) if we ignore the underlying space. However, large L , or the lack of global interactions, permits the disease to spread only linearly in time [13]. This contrasts with a small-world type of networks and fully mixed networks like random graphs in which diseases spread exponentially fast in the beginning [3, 21]. Accordingly, the transmission is by far slower than shown in Fig. 2(a, b, c, d). Although propagations at linear rates would be good approximation before long-range transportations had become readily available, they do not match the recent spreads mediated by long-distance travelers that lessen L [2, 6, 9, 19]. Taken in another way, restrictions on long movements can be a useful spread control [2]. By the same token, mathematical approaches such as percolations and contact processes on regular lattices, which often yield valuable rigorous results [13, 14, 17], are subject to this caveat.

B. Comparison with Scale-free Networks

Another candidate for the network architecture is scale-free networks whose distributions of k_i obey the power laws [10]. Compared with the class of small-world networks [9], scale-free networks, particularly with the original construction algorithm, lack the clustering property, whereas they realize the power law often present in nature [15]. The chains of infection in a scale-free network with the mean vertex degree equal to the previous simulations are shown in Fig. 2(h) and Fig. 2(i) for $\bar{t} = 1.0$ and $\bar{t} = 2.0$, respectively. Compared with the case of our transmission model (see Fig. 2(a, b, c, d)), the influence of SSs is more magnified. Figure 3(b), plotting the distributions of a_i for $\bar{t} = 2.0$, shows that the distribution of a_i decays with a power law rather than exponentially for small a_i . When more extensive data become available, we will be able to fit Fig. 3(a) or Fig. 3(b) to the real data as shown in Fig. 3(c) and gain more insights into the real epidemics, based on the distributions of a_i . Figure 3 also suggests that more patients in total result from the epidemics in scale-free networks than in our model network, even though the mean transmission rate and the mean vertex degree are the same.

In Fig. 4, we plot (k_i, a_i) for each subpopulation of the susceptible ($a_i = 0$), the infected non-SSs, and the SSs. For the infected non-SSs and the SSs, a_i is roughly proportional to k_i . This explains the power-law tail in Fig. 3(b) and enables the existence of extremely contagious SSs that could be called ultra-superspreaders. The scale-free property implies highly heterogeneous distribution of k_i . Compared with the same size of regular, small-world, or random networks whose k_i s are relatively homogeneous, scale-free networks have larger $R_0 \propto \langle k_i^2 \rangle / \langle k_i \rangle$ [3, 8, 12, 16]. In percolation models, $R_0 = \sum_{i=0}^n k_i(k_i - 1)\lambda_i$, where λ_i denotes the rate of possible transmission from the i th individual [8]. Consequently, in the original scale-free networks whose density function of k_i is proportional to k_i^{-3} , the critical value present for regular, small-world, or random networks of the same mean edge density is extinguished [8]. The same is true for dynamical models such as contact processes [12]. Accordingly, scale-free networks spread diseases even with infinitesimally small infection rates. Furthermore, if a positive critical value exists with the type of scale-free networks whose distribution of k_i follows k_i^γ ($\gamma < -3$), a tendency that SSs occupy vertices with large k_i can remove the critical values. For example, the critical infection rate shrinks to 0 if $\lambda_i \propto k_i^{\gamma'}$ with $\gamma' > -\gamma - 3$.

Does this mechanism underlie the current and possible spreading of SARS? We think not, firstly because SSs do not necessarily seem to prefer to inhabit hubs of networks. Even without such correlation, heterogeneous infection strengths of patients are not probably determined by the highly heterogeneous k_i . A major route for SARS transmission is daily personal contacts. In this respect, distributions of k_i of acquaintance networks and friendship networks do not follow power laws but have exponential tails because of aging of individuals and their limited capacity [15, 16]. Particularly, the number of contacts per day is limited by the time and the energy of a person, which flattens the distribution of k_i ; SSs of SARS seem to lead ordinary social lives. SSs possibly result from the combination of large λ_i and the stay in groups with large $\langle k_i \rangle_j T_j$, as has been discussed in this paper. Scale-free networks are rather relevant to spreads of computer viruses and STDs [11, 12, 16, 19]. Spreads are mostly mediated by individuals on hubs in such epidemics, and ultra-superspreaders may result as a combination of large λ_i and large k_i [3, 19]. Preventive efforts to target active patients with large k_i are effective in these diseases [8]. However, efforts to suppress SARS should be invested

in identifying the patients with large λ_i and places with large $\langle k_i \rangle_j T_j$, rather than in looking for socially active persons that exist only with probability exponentially small in k_i .

C. Effects of Clustering

A bonus of using a small-world type of networks is that they are clustered, as measured by the cluster coefficient C [9]. In the real situations, the probability that two patients directly infected by the same patient know each other is significantly high. Also from this viewpoint, small-world networks are more relevant than networks with small C such as scale-free networks or random graphs. We have used the network shown in Fig. 1 instead of the model by Watts and Strogatz [9] to facilitate analysis and comprehensive understanding of the dynamics. With edges appearing in different timings superimposed, $C \cong \langle k_i \rangle / n_g c$ where c is the number of random groupings ($c = 2$ in our simulations), whereas $L \propto \log n$. If k_i is the order of n_g and c is not so large, our network has small-world properties characterized by large C and small L .

The notion of clustering might induce one to imagine situations in which people congregate and SARS spreads. However, infection occurs only on the boundaries between a susceptible and a patient, and propagation slows if a pair of the infected face each other as typically happens in highly clustered networks. Increase in C rather elevates the epidemic threshold in site percolations [21, 22], bond percolations [8, 22], and contact processes [7, 9, 13]. It also decreases the final size of the infected population, or spreads in late stages [7, 9]. In spite of these general effects of C , however, we claim that C does not count in the outbreak of SARS. The possibility of outbreaks and dynamics in initial stages are determined by other factors such as λ_i , k_i , T_j , and σ . If the i th individual that happens to be a patient has \bar{k} neighboring patients, the effective k_i decreases to $k_i - \bar{k}$. However, \bar{k} is tiny relative to k_i in early stages even if C is large. On the other hand, clustering in the sense of large C indirectly promotes the spreads by increasing k . The arguments above on the effects of C are based on varying C with k fixed. However, the population density of a group concurrently modulates k and C [3]. In a group of n_g people with spatial size S_g , $\langle k_i \rangle = (n_g - 1)S_p/S_g$, where S_p is the size of personal space within which each person randomly interacts with others. Obviously,

$\langle k_i \rangle$ is proportional to the population density n_g/S_g . In addition, $C = S_p/S_g \propto \langle k_i \rangle$ even for a fully mixed population. Therefore, the concept of clustering related to the SARS spreads is high population density. The network with large C has been applied in this paper to respect the social reality.

V. CONCLUSIONS

In this paper, we have proposed a dynamic network model for SARS epidemics and shown that combined effects of super-spreaders and their possible tendencies to haunt potentially contagious places can amplify the spreads. In addition, we have contrasted the different dynamical consequences according to different types of underlying network structure.

Acknowledgments

We thank M. Urashima for helpful discussions. This study is partially supported by the Japan Society for the Promotion of Science and also by the Advanced and Innovative Research Program in Life Sciences from the Ministry of Education, Culture, Sports, Science, and Technology, the Japanese Government.

-
- [1] M. Lipsitch et al. *Science* **300**, 1966 (2003).
 - [2] S. Riley et al. *Science* **300**, 1961 (2003).
 - [3] R. M. May, R. M. Anderson. *Nature* **326**, 137 (1987); *Phil. Trans. R. Soc. Lond. B* **321**, 565 (1988).
 - [4] Y. S. Leo et al., *MMWR* **52**, 405 (2003).
 - [5] G. Vogel. *Nature* **300**, 558 (2003).
 - [6] A. S. M. Abdullah, B. Tomlinson, C. S. Cockram, G. N. Thomas. *Emerging Infectious Diseases* **9**, 1042 (2003).
 - [7] M. J. Keeling. *Proc. R. Soc. Lond. B* **266**, 859 (1999).
 - [8] M. E. J. Newman, *Phys. Rev. E* **66**, 016128 (2002).

- [9] D. J. Watts, S. H. Strogatz. *Nature* **393**, 440 (1998); D. J. Watts. *Small Worlds* (Princeton University Press, Princeton, 1999).
- [10] A.-L. Barabási, R. Albert. *Science* **286**, 509 (1999).
- [11] F. Liljeros et al. *Nature* **411**, 907 (2001).
- [12] R. Pastor-Satorras, A. Vespignani. *Phys. Rev. Lett.* **86(14)**, 3200 (2001).
- [13] R. Durrett. *Lecture Notes on Particle Systems and Percolation* (Wadsworth, Inc., California, 1988).
- [14] R. B. Schinazi. *Mathematical Biosciences* **173**, 25 (2001).
- [15] L. A. N. Amaral, A. Scala, M. Barthélémy, H. E. Stanley. *Proc. Natl. Acad. Sci. USA* **97(21)**, 11149 (2000).
- [16] A. L. Lloyd, R. M. May. *Science* **292**, 1316 (2001).
- [17] T. M. Liggett. *Interacting Particle Systems* (Springer, New York, 1985); R. B. Schinazi. *Classical and Spatial Stochastic Processes* (Birkhäuser, Boston, 1999).
- [18] D. J. Watts, P. S. Dodds, M. E. J. Newman. *Science* **296**, 1302 (2002).
- [19] R. M. May, A. L. Lloyd. *Phys. Rev. E* **64**, 066112 (2001).
- [20] L. W. Ancel, M. E. J. Newman, M. Martin, S. Schrag. Santa Fe Institute Report, No. 01-12-078 (2001).
- [21] M. E. J. Newman, D. J. Watts. *Phys. Rev. E* **60(6)**, 7332 (1999).
- [22] C. Moore, M. E. J. Newman. *Phys. Rev. E* **61(5)**, 5678 (2000).

Figure captions

Figure 1: Schematic diagram of the dynamic network for $n_g = 4$ and $g = 4$. The vertices initially form random graphs within each group. After time t_0 , they are randomly shuffled to reform new groups. The graph switches between the two configurations with period t_0 .

Figure 2: Chains of infection in the dynamical small-world network (a, b, c, d), the two-dimensional regular lattice (e, f, g), and the scale-free network (h, i). Transmissions from the infected non-SSs and those from SSs are shown by dashed and solid lines, respectively. We set $n = 90^2$, $n_g = 81$, $g = 100$, $\lambda_I = 0.026$, $\lambda_{SS} = 0.52$, $k = 80$, and the time step $\Delta t = 0.05$. We set $t_0 = 0.5$ and $\bar{t} = 1.0$ in (a, b), $t_0 = 0.5$ and $\bar{t} = 2.0$ in (c), $t_0 = 1.0$ and $\bar{t} = 2.0$ in (d), $\bar{t} = 1.0$ in (e, h), $\bar{t} = 2.0$ in (f, i), and $\bar{t} = 3.0$ in (g). (a) and (b) correspond to the two groupings shown in Fig. 1. In (e, f, g), a square lattice with 90×90 vertices are used, and $k = 80$. In (h, i), the scale-free network with $k = 80$ and $n = 90^2$ is generated by starting with a complete graph of 40 vertices and adding $n - 40$ vertices. Each vertex is endowed with 40 new edges whose destinations are determined according to preferential attachment [10].

Figure 3: Distributions of a_i , namely, the number of individuals to whom a patient has directly infected, in (a) the dynamical small-world network, (b) the scale-free network, and (c) Singapore [4]. The distributions are shown for the SSs (crosses) and all the patients (circles). We set $\bar{t} = 2.0$ in (a, b) and $t_0 = 0.5$ in (a).

Figure 4: Relation between the vertex degree k_i and the number of infections a_i in the scale-free network for the susceptible (squares), the infected non-SSs (crosses), and the SSs (circles), with the numerical data used for Fig. 3(b).

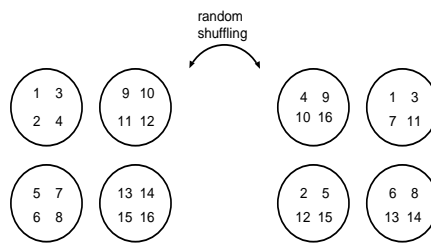


FIG. 1:

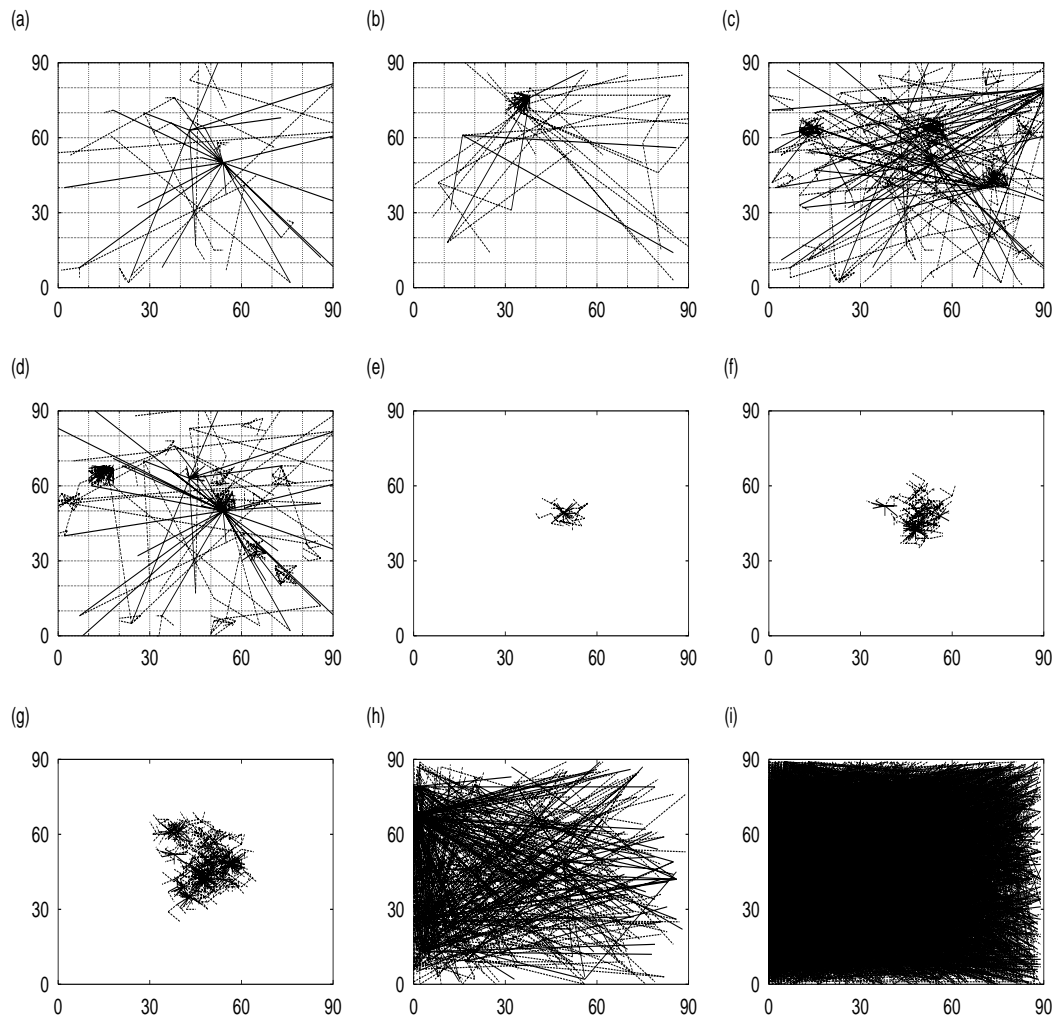


FIG. 2:

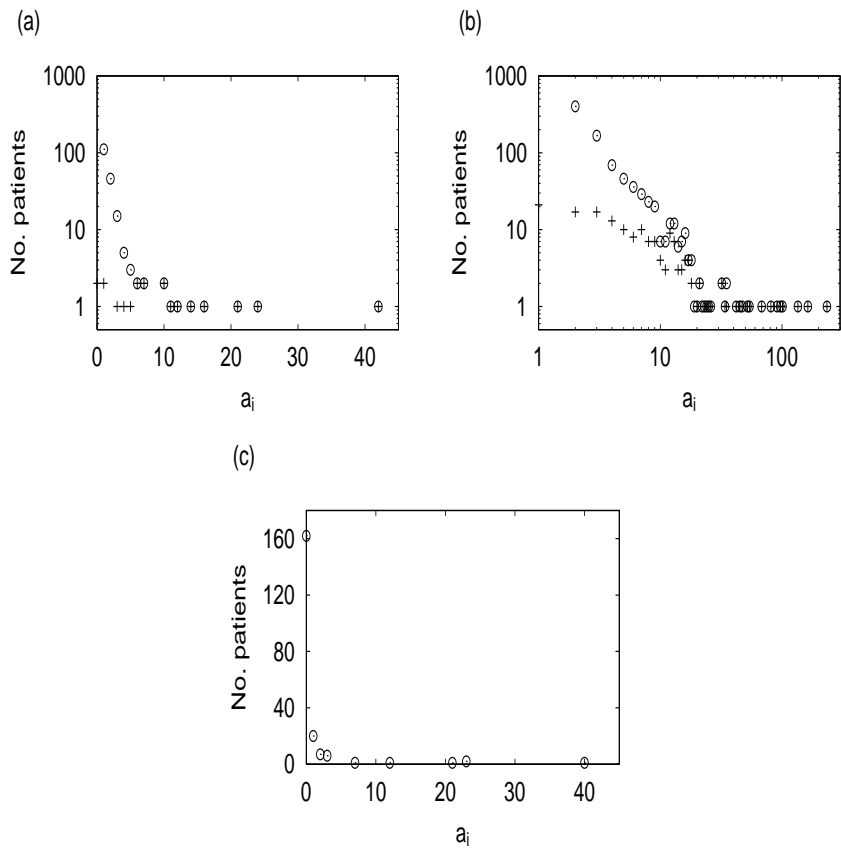


FIG. 3:

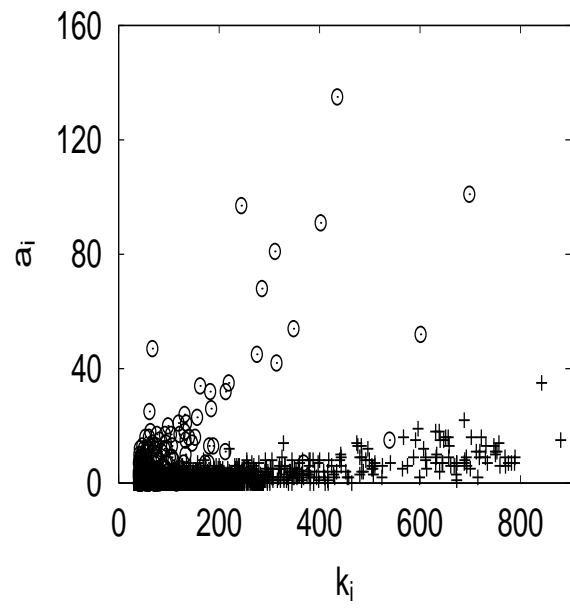


FIG. 4: